Author's Accepted Manuscript

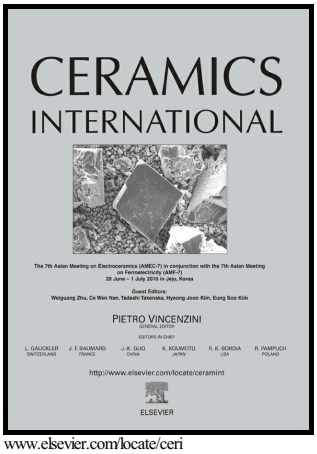

www.elsevier.com/locate/ceri

Improved Transparency and Hardness in α-alumina Ceramics Fabricated by High-pressure SPS of Nanopowders

Shaghayegh Ghanizadeh, Salvatore Grasso, Prabhu Ramanujam, Bala Vaidhyanathan, Jon Binner, Peter Brown, Judah Goldwasser

PII: S0272-8842(16)31683-2
DOI: http://dx.doi.org/10.1016/j.ceramint.2016.09.150
Reference: CERI13810

To appear in: *Ceramics International*

Received date: 25 August 2016
Revised date: 20 September 2016
Accepted date: 21 September 2016

Cite this article as: Shaghayegh Ghanizadeh, Salvatore Grasso, Prabhu Ramanujam, Bala Vaidhyanathan, Jon Binner, Peter Brown and Judah Goldwasser, Improved Transparency and Hardness in α-alumina Ceramics Fabricated by High-pressure SPS of Nanopowders, *Ceramics International* http://dx.doi.org/10.1016/j.ceramint.2016.09.150

This is a PDF file of an unedited manuscript that has been accepted for publication. As a service to our customers we are providing this early version of the manuscript. The manuscript will undergo copyediting, typesetting, and review of the resulting galley proof before it is published in its final citable form. Please note that during the production process errors may be discovered which could affect the content, and all legal disclaimers that apply to the journal pertain.

ACCEPTED MANUSCRIPT

Improved Transparency and Hardness in α-alumina Ceramics Fabricated by High-pressure SPS of Nanopowders

Shaghayegh Ghanizadeh[a†], Salvatore Grasso[b], Prabhu Ramanujam[c], Bala Vaidhyanathan[a], Jon Binner[c], Peter Brown[d], Judah Goldwasser[e]

[a] Department of Materials, Loughborough University, Loughborough, LE11 3TU, UK

[b] Queen Mary, University of London, London, E1 4NS, UK

[c] School of Metallurgy and Materials, College of Engineering and Physical Sciences, University of Birmingham, Edgbaston, Birmingham, B12 2TT, UK.

[d] Dstl, Porton Down, Salisbury, SP4 0JQ, UK

[e] ONRG, Middlesex, HA4 7HB, UK

[†] Corresponding author: Shaghayegh Ghanizadeh, Email address: s.ghanizadeh@lboro.ac.uk (Now with the Wolfson School of Mechanical, Electrical and Manufacturing Engineering, Loughborough University).

Accepted manuscript

Abstract

Nanocrystalline alumina powder with an average crystallite size of ≤50 nm has been consolidated by spark plasma sintering (SPS) and hot pressing (HP) with a view to achieving dense, fine grained alumina bodies that display transparency. When as-synthesised powder was densified directly, excessive grain growth resulted from both the SPS and HP techniques and hence a large final grain size was observed. Attempts to improve the uniformity of the green microstructure prior to densification were unsuccessful when spray freeze dried granules were used, whether pre-pressed into a compact or not. The use of 53% dense slip cast green compacts, however, enabled final density of ~99.96% and a mean grain size of ~0.32 μm to be achieved when SPS conditions of 1200˚C and 500 MPa were

ACCEPTED MANUSCRIPT

applied for 20 minutes. These samples offered in-line transmittance values of up to ~80% and microhardness values of 22 GPa.

Keywords: Nanocrystalline; Alumina; SPS; Hot press; Transparent

1. Introduction

Nanocrystalline ceramics typically have a mean grain size of <100 nm. The motivation for manufacturing and studying such ceramics lies in their potential to yield unusual and useful properties such as superplasticity, high hardness and extremely low thermal conductivity [1-5]. Owing to its combination of high hardness, corrosion resistance, thermodynamic stability and relatively low cost alumina is the most common engineering ceramic. It is used for a very wide range of applications, including armour, hip implants, thread guides, cutting tools, valves, water tap mixers and many other applications [6]. One particular advantage offered by very fine grain size alumina is that it is transparent when the final density is ≥99.95% of theoretical and the mean grain size is below ~1 μm [7]. It should be noted, however, that, unlike ceramics with cubic crystal structures, polycrystalline alumina is birefringent [8]. Hence mean grain sizes smaller than the incident light wave length are needed to limit scattering losses and achieve true transparency [8]. For example, Krell, et al. [9] fabricated alumina with 99.9% of theoretical density and a mean grain size of ~0.5 μm, with 0.8 mm thick samples exhibiting real in-line transmissions (RIT) of 60% at a wavelength of 650 nm [9].

Highly dense, submicron, transparent ceramics have traditionally been obtained using either hot pressing or hot isostatic pressing of fine, submicron powders. More recently, spark plasma sintering has been investigated as a tool for achieving even finer microstructures. Essentially similar to hot pressing, the method of heating used – the passage of an electric current through a graphite die set – results in heating rates as high as 10^6 K s^{-1}, lower sintering temperatures and reduced time at temperature [10-12]. For example, fully dense

Accepted manuscript

alumina bodies with a mean grain size of 0.5 μm were obtained at only 1200˚C with dwell times of 3-10 minutes by SPS [13,14]. Grasso et al. [15,16] fabricated transparent, pure alumina bodies by densifying commercial alumina powder with a crystallite size of 130-200 nm at temperatures as low as 1000˚C under 500 MPa. Fully dense, fine grained alumina with porosity <0.05% was obtained with an in-line transmission of about 64% at a wavelength of 645 nm [17]. Use of dopants such as La^{3+} has also been investigated to fabricate highly dense transparent ceramics with 71% real in-line transmission (at 640 nm) using slip cast samples prepared from commercial ultrafine alumina doped with La^{3+} using SPS to achieve densification [18].

In this work, it is shown that high-pressure spark plasma sintering using an in-house synthesised nano α-alumina powder, with an initial particle size of ≤50 nm, can lead to the formation of dense transparent alumina bodies with transmittance values of ~80%. The effect of employing different green forming methods, including slip casting and spray freeze granulation, has been investigated. Hot pressing, an alternative pressure-assisted technique, has also been used to compare the densification processes.

2. Materials and methods

The powder used was pure α-alumina nanopowder with a specific surface area of ~35 m^2g^{-1} and average crystallite size of ≤50 nm. Details of the synthesis method are provided elsewhere [19,20], but, in brief, the powder was synthesised from an aluminium chloride and ammonia solution using a precipitation-based method followed by a two-step heat treatment route to prevent the high degree of agglomeration occurring during conversion of the precursors into metal oxides [21].

Green forming: 60 wt% solids content nanoalumina suspensions were produced by mixing appropriate quantities of deionised water and an anionic polyelectrolyte (Dolapix CE-64,

Accepted manuscript

ACCEPTED MANUSCRIPT

Zschimmer & Schwarz GmbH, Lahnstein, Germany) as a dispersant and stirring for 1 hour. The nanoalumina powder, weighed to 0.01 g, was added subsequently and the mixture ball-milled for 12 hours using alumina balls to achieve an homogeneous suspension. This was subjected to ultrasonic agitation (SoniPrep, MSE Ltd, London, UK) for 3 minutes whilst placed in a water bath, using 150 W at 15 kHz in clean glass beakers, whilst the after which the latter were sealed using Parafilm to prevent water evaporation and left for 1 hour to cool and attain equilibrium. Finally, the samples were held at a reduced pressure of 60 mm mercury for 10 minutes to remove as many air bubbles as possible.

Slip casting was performed using a 15 mm thick acrylic sheet with an array of nine 15 mm diameter drilled holes, clamped to a ~50 mm thick flat plate of Plaster of Paris, PoP (Prestia 23 casting plaster, Lafarge, Cambridgeshire, UK), Figure 1. The latter was produced using a PoP-to-water ratio of 60:40. Lubricant (silicone spray; Ambersil, CRC Industries UK Ltd, Bridgwater, UK) was applied to the inside surfaces of the holes in the acrylic sheet to ease green body removal followed by the suspension being cast into them. This approach allowed up to 9 samples to be slip cast simultaneously, the dewatering process occurring into the plaster plate beneath the acrylic sheet. Drying of the cast green bodies was carried out under ambient conditions of ~20ºC and 50% humidity for 72 hours before samples were removed from the acrylic sheet with great care. Following this preliminary drying, all the samples were placed on a Teflon sheet for further drying at 60^{o}C in an oven; the Teflon sheet assisted with sample shrinkage by providing minimal resistance.

Granulated powders were also produced from a similar slurry to that used above by spraying the suspension into liquid nitrogen followed by drying the frozen granules in a freeze dryer. This suspension included 2 vol. % Freon 11 (Spex CertiPrep. Inc, UK) as a foaming agent to weaken the granules and 0.5 wt% PVA (Fluka, UK) as a pressing binder. Spraying was performed using a twin fluid atomiser (BÜCHI Labortechnik AG, Postfach, Switzerland); the suspension flow rate was controlled via a compressed air flow from a VT 150 air compressor

Accepted manuscript

(Bambi Air Compressors Ltd, Birmingham, UK) using a flowmeter. Once the excess nitrogen had evaporated off, the frozen granules were freeze dried in a benchtop freeze drier (Virtis® Benchtop SLC, New York, USA). The process of freeze drying took at least 48 hours, depending on the amount of sample required to be dried. As a final step, sieving was undertaken to extract the fraction between 125 and 250 μm to maximise the flowability [22]. Dry pressing was carried out using a Lloyds mechanical testing machine (L10000 Tensometer, Lloyds Instruments, Fareham, UK) in a single-action, hardened steel die with a diameter of 10 mm. About 0.5 g of powder was used for each pellet, which was pressed at 480 MPa for 1 minute.

Removal of the organics present in both slip cast and die pressed green bodies was achieved by heating at a rate of 0.5°C min^{-1}, with dwells at 100°C, 200°C, 300°C and 400°C for 30 minutes each, and finally at 700°C for 2 hours before being cooled down to room temperature at a rate of 0.5°C min^{-1}. After the binder removal stage, all the samples were visually inspected for the presence of any defects such as cracks. The relative density of both slip cast and die pressed bodies was measured after binder removal by both the Archimedes technique using mercury and by measurement of mass and volume.

Hot pressing (HP): The as-synthesised nanoalumina powder was directly hot pressed using the facility at the University of Exeter, UK (8538 UEO, Systeme GmbH, Frankenblick, Germany). The powder was poured into the die, tapped to a level surface and then heated initially under vacuum until 900˚C and then in argon; the heating rate was 10˚C min^{-1} for all the experiments. When the temperature reached the desired sintering value, in the range 1400-1700˚C, see Table 1, an external pressure of 40 MPa was applied to both ends of the die using graphite plungers; this remained constant throughout the sintering process, which lasted 5 hours. Subsequently, the load was removed and the samples were left to cool down. Samples of 50 (length) × 50 (breadth) × 2.4 (height) mm were obtained after densification.

Accepted manuscript

Spark plasma sintering (SPS): Work started with the direct spark plasma sintering of as-synthesised nanoalumina powder using the facility at Queen Mary University, UK (FCT HP D 25, FCT Systeme GmbH, Frankenblick, Germany). The conditions used are summarised in Table 1. Two sample sizes were sintered; those densified at 70 MPa were 20 mm in diameter, whilst when 500 MPa or 1000 MPa was used the sample size had to be reduced to 5 mm in diameter. All samples were ~2.5 mm thick after densification. The die used for the two higher pressures was composed of outer and inner graphite dies with SiC punches. The powder was heated under vacuum at a rate of 100˚C min^{-1} to an intermediate dwell point of 700^{o}C, where the pressure was applied. Subsequently, the temperature was raised to the desired sintering temperature, followed by a dwell time of 30 minutes (70 MPa) or 20 minutes (500 MPa and 1000 MPa). Optical pyrometery was used to measure the temperature; it was focused on a hole that penetrated halfway through the inner graphite die. The sintering kinetics were monitored from the variation of the total height of the graphite die assembly with temperature. The applied pressure was removed during the cooling cycle, which involved a rate of 100˚C min^{-1}. Additional experiments were performed using the SFD powder which, it was expected, would compact to a higher density when the pressure was applied during the SPS cycle. Subsequently, die pressed and (thoroughly dried) slip cast samples were SPSed, Table 1.

Characterisation: To eliminate the layers affected by heavy carbon contamination from the dies used for both HP and SPS, the surfaces of the sintered samples were removed using a grinding disc with a grit size of 80 and their densities were measured by the Archimedes technique using water. Microstructures were investigated by FEG-SEM (Leo 1530VP FEGSEM, LEO Elektronenskopie GmbH, Oberkochen, Germany) after polishing and thermally etching the samples for 10 minutes at ~100°C below the sintering temperature for each sample. As a typical polishing cycle, mounted samples were initially plain ground using a grinding disc with a grit size of 220 (MD-Piano, Struers Ltd, Solihull, UK), followed by

Accepted manuscript

polishing with 600 and 1200 grit-sized discs (MD-Piano, Struers Ltd, Solihull, UK) using water as the lubricating and cooling media. Subsequent polishing continued using polishing cloths, MD-Plan and MD-Dac (Struers Ltd, Solihull, UK), and stable diamond suspension containing a mixture of high performance diamonds and cooling lubricants, DP-Plan and DP-Dac (Struers Ltd, Solihull, UK), consisting of particles of 9 μm and 3 μm in size, respectively.

At least 300 grains were measured in each of three micrographs to determine the mean grain size for each alumina sample. The average grain size was calculated using the equation:

$$D = \frac{L \times A_l}{M \times N} \qquad \text{Eq. 1}$$

where D is the equivalent average grain diameter, L is the length of the superimposed lines, A_1 is a shape correction factor of 1.56 used to convert the two dimensional grain size to three dimensional [23], M is the magnification and N is the number of intercepts or intersections.

All the disks were polished to a mirror finish on both sides for optical characterisation using the conditions outlined above. The in-line transmission of the samples was measured using a Shimadzu Fourier Transform Infrared spectrometer (FTIR 8400S, Shimadzu, Tokyo, Japan) for the infrared range of 2.5-10 μm and a UV-VIS double-beam spectrometer (Lambda 35, Perkin Elmer, Shelton, USA) for the visible range of 300-800 nm.

The microhardness of the sintered bodies was determined after polishing using the approach described in ASTM E 384 (HM-124 micro hardness tester, Mitutoyo Corporation, Kawasaki, Japan). A square-based pyramidal diamond indenter with face angles of 136° was used by applying a load of 1 kg for 15 seconds. After removing the load, the lengths of the diagonals of the indentation on the sample were measured via a microscope and the Vickers hardness of the samples calculated using:

$$HV = 0.0018544 \times P/d^2 \qquad \text{Eq. 2}$$

Accepted manuscript

where HV is the Vickers hardness in GPa, P is the applied load in N, and d is the length of the long diagonal of the indentation in mm.

3. Results and Discussion

Figure 2 shows the fracture surfaces of green slip cast and die pressed bodies with density values of ~53% of theoretical density. The latter was pressed using granulated powders at 480 MPa. Lower level of agglomeration was observed on both fracture surfaces particularly for the slip cast compact; this could be due to the improved dispersion of alumina nanopowder in the suspension via breaking up the agglomerates using an appropriate dispersant as well as a further sonication step.

3.1. Hot pressing

The density and mean grain size values of the sintered bodies made using the as-synthesised powder are shown in Table 2. Although hot pressing at both 1600˚C and 1700˚C yielded translucent compacts with relative densities of ~99.9%, the bodies possessed coarse microstructures, with average grain sizes of ≥7 μm and grains of over 10 μm frequently being observed, Figure 3. Further work on hot pressing was therefore discontinued.

3.2. Spark plasma sintering

Table 2 also shows the relative density and mean grain size values of the bodies sintered using SPS and produced directly from the as-synthesised nanoalumina powder. As expected, by increasing the pressure up to 500 MPa, higher relative densities and lower mean grain sizes were achieved and at lower temperatures compared to samples compacted at 70 MPa. The use of 1400˚C/70 MPa (SPS-70-14) and 1200˚C/500 MPa (SPS-500-12) both led to alumina bodies with densities of ~99.9% of theoretical density and, consequently, these compacts displayed a degree of translucency, as shown in Figure 4a & b. Note, however, that sample SPS-70-14 had a mean grain size of ~6 μm and some grains of >10 μm, Figure

Accepted manuscript

4c, whilst for SPS-500-12 it was approximately one tenth this size, Figure 4d. Nevertheless, it will be observed that some larger grains were still visible. Unevenness in the compact colour, which is usually caused by carbon contamination occurring during spark plasma sintering, was observed for SPS-70-14 as for the hot pressed samples.

The experiment that involved the use of 1 GPa led to a final density of only ~99.5% of theoretical; this was due to the temperature being limited to only 900˚C by the properties of the graphite used for the die. As a result, the body was opaque, but the mean grain size, at 200 nm, was extremely fine, Figure 5.

The unevenness in the grain size of these samples could be induced by the presence of agglomeration in the as-synthesised powder [19]. It is well known that agglomerates, which are denser than the surrounding matrix, progress up the sintering curve faster leading to excessive grain growth and the solution is to ensure that the packing of the particles is as uniform as possible [24]. Hence spray freeze dried, SFD, granules were produced for subsequent densification using SPS, both as a loose granulated powder and as pre-compacted bodies. However, use of SFD powders resulted in lower final densities compared to the densification of the as-synthesised powder, Table 2 and hence this approach was discontinued.

Densifying die pressed bodies made from the SFD granules was also unsuccessful; once again the final density was <99% of theoretical and, consequently, the sintered bodies were opaque. The use of slip casting, however, was more successful owing to the superior green microstructures achieved. Sample SPS-500-12-SC achieved 99.9% of theoretical density, whilst also retaining a very fine mean grain size of ~300 nm; half the size of that for sample SPS-500-12. The grain size of the densified body made from the slip cast green compact was also fairly uniform, Figure 6. Consequently, the sample was transparent. Decreasing the

Accepted manuscript

sintering temperature to 1100˚C resulted in translucency since, although the mean grain size, at 250 nm, was finer, the density was lower at ~99.6% of theoretical.

3.3. IR and UV-Vis transmission measurements

Figure 7a shows the UV-Vis transmission spectra for a selection of the samples produced as measured using a UV/VIS spectrophotometer (Lambda 35, Perkin Elmer). The plot also shows the in-line transmission values of alumina compacts investigated in different studies. It can be seen that in the current work the transmittance values increased with increasing wavelength; samples SPS-70-14 and SPS-500-12-SC both had total transmissions of ~75% at 645 nm, whilst the other samples, with their lower densities, exhibited lower transmittances. It also can be seen that the transmittance values over both wavelength ranges are broadly comparable to data measured by other researchers. The data included in Figure 7b presents the IR transmission spectra for the manufactured alumina compacts and, in the inset, for ceramics such as alumina, spinel, yttria and YAG. It can be seen that, as expected, the transmittance was very low, <50%, for the HP samples owing to their very low densities. Samples SPS-70-12, SPS-70-14 and SPS-500-12 all showed very similar behaviour, with maximum transmittance values in the range of 73-75%. Sample SPS-500-12-SC, which had been slip cast, however, showed a higher transmittance of ~80% at ~5 μm, with the cut-off occurring at higher wavelengths. Note, however, that this sample was only ~0.5 mm thick.

3.4. Hardness measurements

Figure 8 shows Vickers microhardness data as a function of mean grain size for the SPS samples. Each data point is an average of at least 10 indents and all the indents were created by applying a 1 kg load.

As can be seen, the hardness values of the samples showed a small increase with decreasing grain size. The reason could be the presence of more grain boundaries in the samples with smaller grain size, restricting the free path of dislocations resulting in a

Accepted manuscript

reduction in plastic deformation [29,30]. It may also be seen that the hardness value of sample SPS-500-12-SC, ~ 22 GPa, was the highest and matched the data in the literature for fully-densified alumina bodies prepared using sub-micrometer powders.

4. Conclusions

Although the use of hot pressing was not successful in the current work, samples made using SPS could be produced with densities up to 99.9% of theoretical. When as-synthesised powder was densified directly, excessive grain growth resulted and hence a large final grain size was observed; ~6.25 µm for sample SPS-70-14 and ~0.64 µm for sample SPS-500-12. The use of spray freeze dried granule powder as a more crushable alternative to as-synthesised powder, whether pre-pressed into a compact or not, failed to result in high enough densities, but the use of slip casting yielded green bodies of 53% density that could subsequently be densified to ~99.96% of theoretical density at 1200˚C/500 MPa, whilst retaining a mean grain size of ~0.32 µm. These samples offered in-line transmittance values of up to ~80%; which approaches the transmission value of sapphire (86%). Microhardness values of 22 GPa were also obtained on reducing the grain size of sintered alumina by applying high pressure during the SPS process; this value is slightly improved in comparison with the values achieved in previous work on pure alumina. Attempts to increase the pressure to 1 GPa or drop the temperature to 1100^{o}C at 500 MPa were unsuccessful, in both cases higher sintering temperatures were needed.

Accepted manuscript

Acknowledgements

Authors would like to thank Professor Mike Reece from Queen Mary University of London and Professor Yanqiu Zhu, Dr. Hong Chang and Dr. Bahareh Yazdani from University of Exeter for providing access to the SPS and hot press facility and Dstl in the UK and ONRG in

ACCEPTED MANUSCRIPT

the USA for funding. The authors would also acknowledge use of facilities within the Loughborough Materials Characterisation Centre (LMCC).

Accepted manuscript

ACCEPTED MANUSCRIPT

References

1. M. Mayo, 'Processing of nanocrystalline ceramics from ultrafine particles,' Int. Mater. Rev., 41 [3] 85-115 (1996).

2. R. M. Piticescu, R. Piticescu, D. Taloi and V. Badilita, 'Hydrothermal synthesis of ceramic nanomaterials for functional applications,' Nanotechnology, 14 [312] 312-317 (2003).

3. W. L. Suchanek and J. M. Garces, 'Hydrothermal synthesis of novel alpha alumina nano-materials with controlled morphologies and high thermal stabilities,', Cryst. Eng. Com., 12 [10] 2996-3002 (2010).

4. T. G. Nieh, J. Wadsworth and F. Wakai, 'Recent advances in superplastic ceramics and ceramic composites,' Int. Mater. Rev., 36 146-161 (1991).

5. J. Karch, R. Birringer and H. Gleiter, 'Ceramics ductile at low temperature,' Nature, 330 [6148] 556-558 (1987).

6. A. Krell and P. Blank, 'The influence of shaping method on the grain size dependence of strength in dense submicrometre alumina,' J. Eur. Ceram. Soc., 16 [11] 1189-1200 (1996).

7. A. Krell, P. Blank, H. Ma, T. Hutzler and M. Nebelung, 'Processing of high-density submicrometer Al_2O_3 for new applications,' J. Am. Ceram. Soc., 86 [4] 546-553 (2003).

8. A. Krell, J. Klimke and T. Hutzler, 'Transparent compact ceramics: Inherent physical issues,' Opt. Mater., 31 [8] 1144-1150 (2009).

9. A. Krell, P. Blank, H. Ma, T. Hutzler, M. P. Bruggen and R. Apetz, 'Transparent sintered corundum with high hardness and strength,' J. Am. Ceram. Soc., 86 [1] 12-18 (2003).

10. J. R. Groza, 'Sintering of nanocrystalline powders,' Int. Powder Metall., 35 [7] 59-66 (1999).

11. J. Langer, M. J. Hoffmann and O. Guillon, 'Direct comparison between hot pressing and electric field-assisted sintering of submicron alumina,' Acta Mater., 57 [18] 5454-5465 (2009).

12. S. Grasso, Y. Sakka and G. Maizza, 'Electric current activated/assisted sintering (ECAS): a review of patents 1906–2008,' Science and Technology of Advanced Materials, 10 [5] 053001 (2009).

13. Z. Shen, M. Johnsson, Z. Zhao and M. Nygren, 'Spark plasma sintering of alumina,' J. Am. Ceram. Soc., 85 [8] 1921-1927 (2002).

14. R. Dobedoe, G. West and M. Lewis, 'Spark plasma sintering of ceramics,' Bull.Eur.Ceram.Soc, 1 [1] 19-24 (2003).

15. S. Grasso, C. Hu, G. Maizza, B. Kim and Y. Sakka, 'Effects of pressure application method on transparency of spark plasma sintered alumina,' J. Am. Ceram. Soc., 94 [5] 1405-1409 (2011).

Accepted manuscript

16. S. Grasso, H. Yoshida, H. Porwal, Y. Sakka and M. Reece, 'Highly transparent α-alumina obtained by low cost high pressure SPS,' Ceram. Int., 39 3243-3248 (2013).

17. S. Grasso, B. Kim, C. Hu, G. Maizza and Y. Sakka, 'Highly transparent pure alumina fabricated by high-pressure spark plasma sintering,' J. Am. Ceram. Soc., 93 [9] 2460-2462 (2010).

18. N. Roussel, L. Lallemant, J. Chane-Ching, S. Guillemet-Fristch, B. Durand, V. Garnier, G. Bonnefont, G. Fantozzi, L. Bonneau and S. Trombert, 'Highly Dense, Transparent α-Al_2O_3 Ceramics From Ultrafine Nanoparticles Via a Standard SPS Sintering,' J Am Ceram Soc, 96 [4] 1039-1042 (2013).

19. S. Ghanizadeh, X. Bao, B. Vaidhyanathan and J. Binner, 'Synthesis of nano α-alumina powders using hydrothermal and precipitation routes: A comparative study,' Ceram. Int., 40 [1] 1311-1319 (2013).

20. S. Ghanizadeh, Synthesis and processing of nanostructured alumina ceramics, Doctoral dissertation (2013).

21.P. Ramanujam, B. Vaidhyanathan, J. Binner, S. Ghanizadeh, C. Spacie, 'Solvothermal nanoYAG synthesis: Mechanism and particle growth kinetics ,' J. Supercrit. Fluids, 107 433-440 (2016).

22. J. Binner, B. Vaidhyanathan, A. Paul, K. Annaporani and B. Raghupathy, 'Compositional Effects in Nanostructured Yttria Partially Stabilized Zirconia,' Int. J. Appl. Ceram. Technol., 8 [4] 766-782 (2011).

23. M. I. Mendelson, 'Average grain size in polycrystalline ceramics,' J. Am. Ceram. Soc., 52 [8] 443-446 (1969).

24. L. Lallemant, G. Fantozzi, V. Garnier and G. Bonnefont, 'Transparent polycrystalline alumina obtained by SPS: Green bodies processing effect,' J. Eur. Ceram. Soc., 32 [11] 2909-2915 (2012).

25. R. Apetz and M. P. B. van Bruggen, 'Transparent Alumina: A Light-Scattering Model,' J. Am. Ceram. Soc., 86 [3] 480-486 (2003).

26. B. Kim, K. Hiraga, K. Morita and H. Yoshida, 'Spark plasma sintering of transparent alumina,' Scr. Mater., 57 [7] 607-610 (2007).

27. Y. Aman, V. Garnier and E. Djurado, 'Influence of green state processes on the sintering behaviour and the subsequent optical properties of spark plasma sintered alumina,' Journal of the European Ceramic Society, 29 [16] 3363-3370 (2009).

28. Suarez M., Fernandez A., Torrecillas R, Mernendez J.L., 'Sintering to Transparency of Polycrystalline Ceramic Materials'; pp. 527 in Sintering of Ceramics – New Emerging Techniques. Edited by Lakshmanan A. (Ed.) 2012.

29. A. Krell, Klimke and T. Hutzler, 'Advanced spinel and sub-μm Al_2O_3 for transparent armour applications,' J. Eur. Ceram. Soc., 29 [2] 275-281 (2009).

Accepted manuscript

ACCEPTED MANUSCRIPT

30. A. Krell and P. Blank, 'Grain size dependence of hardness in dense submicrometer alumina,' J. Am. Ceram. Soc., 78 [4] 1118-1120 (1995).

31. A. Krell, 'Improved hardness and hierarchic influences on wear in submicron sintered alumina,' Mater. Sci. Eng. A, 209 [1] 156-163 (1996).

Accepted manuscript

ACCEPTED MANUSCRIPT

List of tables:

List of figures:

Accepted manuscript

ACCEPTED MANUSCRIPT

Table 1

Sample		T / ˚C	Time / min	Pressure / MPa
HP-40-14	As-synthesised powder	1400	300	40
HP-40-15	As-synthesised powder	1500	300	40
HP-40-16	As-synthesised powder	1600	300	40
HP-40-17	As-synthesised powder	1700	300	40
SPS-70-10	As-synthesised powder	1000	30	70
SPS-70-12	As-synthesised powder	1200	30	70
SPS-70-14	As-synthesised powder	1400	30	70
SPS-500-10	As-synthesised powder	1000	20	500
SPS-500-12	As-synthesised powder	1200	20	500
SPS-1000-9	As-synthesised powder	900	20	1000
SPS-70-14-SFD	Spray freeze dried powder	1400	20	70
SPS-500-12-SFD	Spray freeze dried powder	1200	20	500
SPS-500-12-DP	Die pressed compact	1200	20	500
SPS-500-12-SC	Slip cast compact	1200	20	500
SPS-500-11-SC	Slip cast compact	1100	20	500

Accepted manuscript

ACCEPTED MANUSCRIPT

Table 2

Sample	Relative density / %	Grain size / μm
HP-40-14	97.54 ± 0.09	6.91 ± 0.07
HP-40-15	98.03 ± 0.07	7.83 ± 0.05
HP-40-16	99.92 ± 0.03	9.14 ± 0.09
HP-40-17	99.91 ± 0.03	9.71 ± 0.08
SPS-70-10	93.91 ± 0.06	0.72 ± 0.04
SPS-70-12	99.17 ± 0.12	4.22 ± 0.05
SPS-70-14	99.90 ± 0.05	6.25 ± 0.06
SPS-500-10	99.45 ± 0.04	0.43 ± 0.02
SPS-500-12	99.92 ± 0.03	0.64 ± 0.03
SPS-1000-9	99.53 ± 0.08	0.24 ± 0.06
SPS-70-14-SFD	98.51 ± 0.05	1.95 ± 0.09
SPS-500-12-SFD	98.80 ± 0.03	0.70 ± 0.04
SPS-500-12-DP	98.92 ± 0.1	0.66 ± 0.09
SPS-500-12-SC	99.96 ± 0.02	0.32 ± 0.07
SPS-500-11-SC	99.67 ± 0.08	0.25 ± 0.07

Accepted manuscript

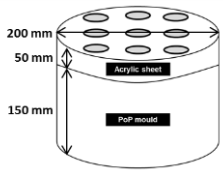

Accepted manuscript

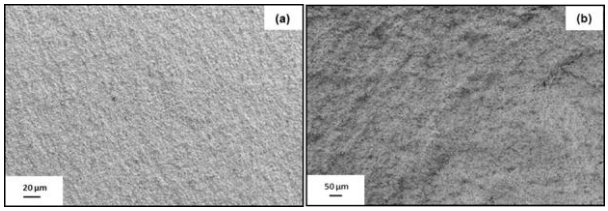

Accepted manuscript

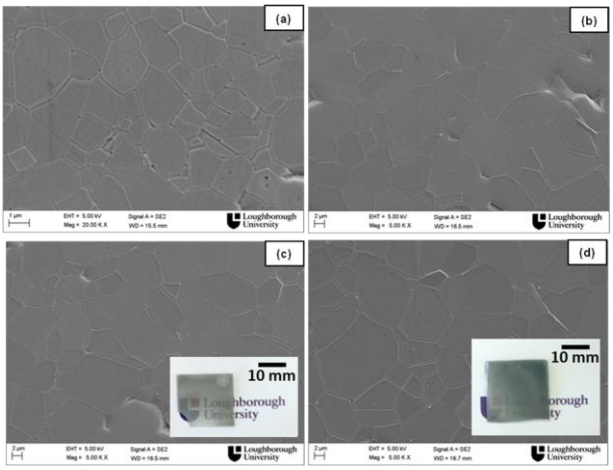

Accepted manuscript

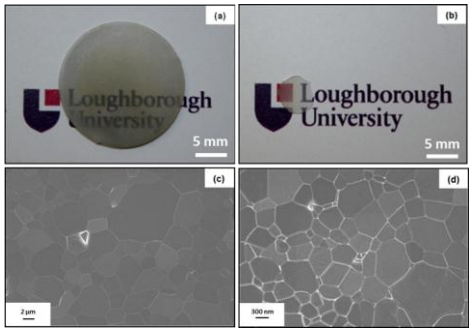

Accepted manuscript

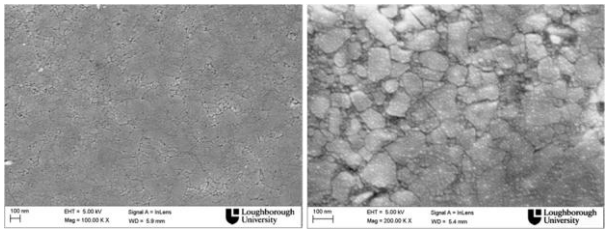

Accepted manuscript

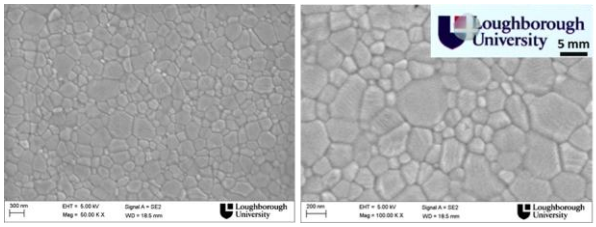

Accepted manuscript

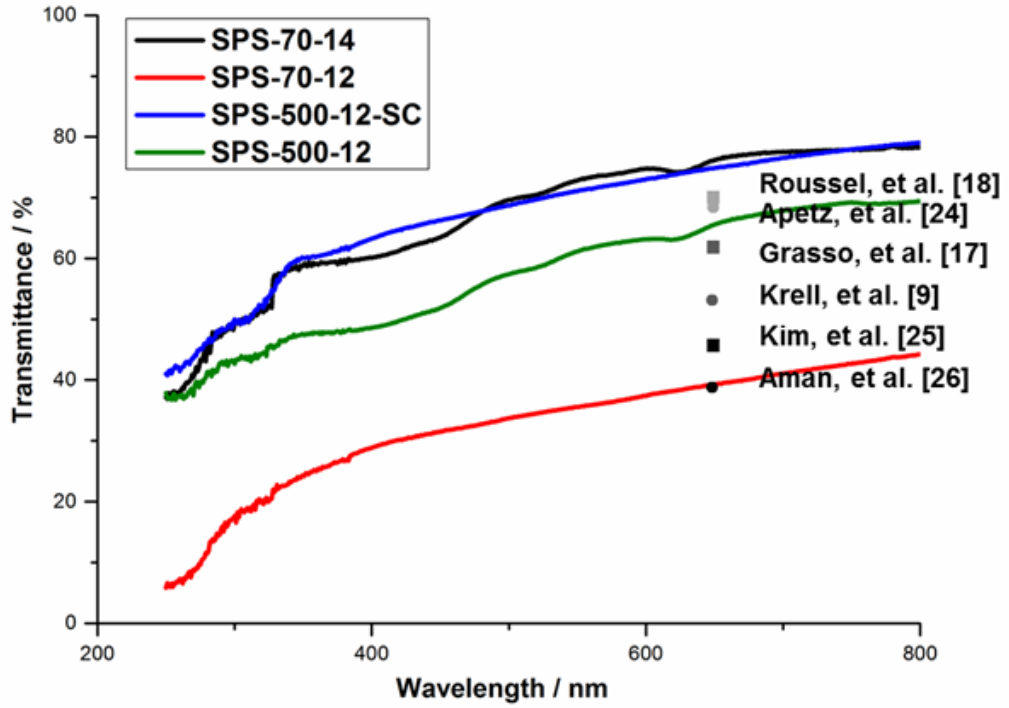
SPS-70-14
SPS-70-12
SPS-500-12-SC
SPS-500-12
Roussel, et al. [18]
Apetz, et al. [24]
Grasso, et al. [17]
Krell, et al. [9]
Kim, et al. [25]
Aman, et al. [26]
Transmittance / %
Wavelength / nm
0
20
40
60
80
100
200
400
600
800

(a)

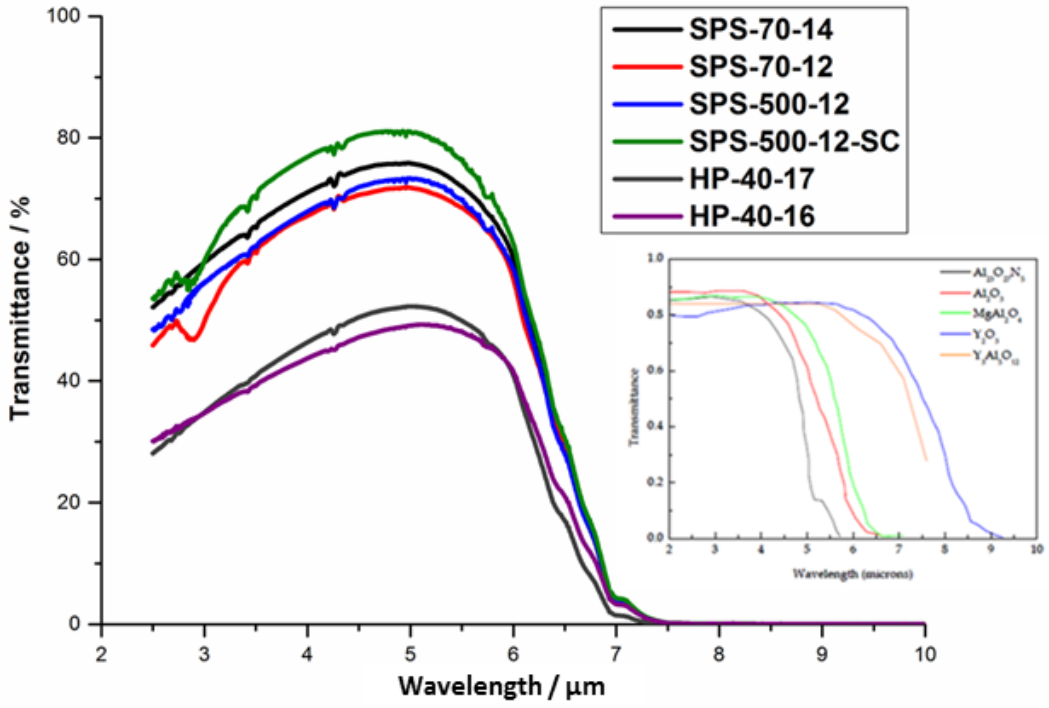
SPS-70-14
SPS-70-12
SPS-500-12
SPS-500-12-SC
HP-40-17
HP-40-16
Transmittance / %
Wavelength / µm
0
20
40
60
80
100
2
3
4
5
6
7
8
9
10

(b)

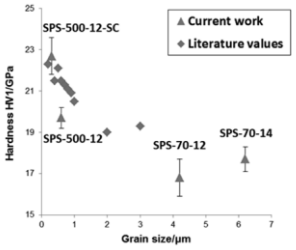

Accepted manuscript